Hindawi Publishing Corporation
Mathematical Problems in Engineering
Volume 2013, Article ID 208753, 9 pages
http://dx.doi.org/10.1155/2013/208753

Research Article

A Study on Control Strategy of Regenerative Braking in the Hydraulic Hybrid Vehicle Based on ECE Regulations

Tao Liu, Jincheng Zheng, Yongmao Su, and Jinghui Zhao

School of Automobile Engineering, Harbin Institute of Technology, Weihai 264209, China

Correspondence should be addressed to Jincheng Zheng; zhengjincheng.com@163.com

Received 1 July 2013; Revised 19 August 2013; Accepted 27 August 2013

Academic Editor: Hui Zhang

This paper establishes a mathematic model of composite braking in the hydraulic hybrid vehicle and analyzes the constraint condition of parallel regenerative braking control algorithm. Based on regenerative braking system character and ECE (Economic Commission of Europe) regulations, it introduces the control strategy of regenerative braking in parallel hydraulic hybrid vehicle (PHHV). Finally, the paper establishes the backward simulation model of the hydraulic hybrid vehicle in Matlab/simulink and makes a simulation analysis of the control strategy of regenerative braking. The results show that this strategy can equip the hydraulic hybrid vehicle with strong brake energy recovery power in typical urban drive state.

1. Introduction

Regenerative braking is an important technology of the hybrid vehicles that appeals to very strong research interests all over the world [1–5]. Research on control strategy is one of most important topics of regenerative braking and can be roughly categorized into two types according to the propose of research. One is to enhance the braking performance and driving comfort. The other is to improve the regenerative efficiency and to save resources. Almost the present research concentrates on regenerative braking in many of electric vehicles (EV), hybrid electric vehicles (HEV), and plug-in hybrid electric vehicles. A mass of solutions in regenerative braking system control have been carried out. For example, Kim et al. [6] and Peng et al. [7] put forward two regenerative braking strategies based on the fuzzy control to pursue high regenerative efficiency and good braking performance. The simulation results indicated that both regenerative braking control strategies could increase the fuel economy for HEV and improve vehicle stability. Oh et al. [8], Jo et al. [9], Zhang et al. [10], Moreno et al. [11], and others have carried out research studies in this field as well. Nevertheless, pieces of the literature devoted to hydraulic hybrid vehicle (HHV) are relatively scarce. Wu et al. [12] proposed a strategy for passenger cars based on dividing the accumulator volume into two parts, one for regeneration and the other for road-decoupling. Hui et al. [13] presented a fuzzy torque control strategy based on vehicle load changes for real-time controlling the energy distribution in PHHV. Though they proposed a methodology of braking to improve the fuel economy in a typical urban cycle, the braking characteristics were not investigated deeply. What is more, the efficiency of brake energy recovery and the distribution of braking force were not considered and optimized at all. The design of regenerative braking strategy in HHV remains a problem yet. Compared with electrified vehicles, HHV has some advantage, particularly for vehicles containing hydraulic equipment on board [14]. For instance, hydraulic accumulator is of higher power density and ability to accept the high rates and high frequencies of charging and discharging [15]. Besides, the service life of a hydraulic accumulator as the storage is more than a battery. Therefore, HHV has a greater potential than electrified vehicles, and the research on that makes much sense. Generally, there are two types of hydraulic hybrid systems: parallel hydraulic hybrid vehicle (PHHV) and series hydraulic hybrid vehicle (SHHV). PHHV uses a traditional mechanical drive train with hydraulic pump/motor unit inline between the transmission and axle [16]. The configuration of PHHV is simpler than that of SHHV and easier to be refitted. Therefore, PHHV occupies large proportion of HHV at home and abroad.

However, it is hard for PHHV driven by rear wheel to obtain a good braking stability as well as an effective regenerative energy recovery. One reason for this phenomenon is that the rear wheel is easy for locking when the hydraulic regenerative braking force is exerted on the back axle. Therefore, when the hydraulic braking force is strong enough, the back-axle utilization adhesion curves may surpass the constraint of ECE (Economic Commission of Europe) regulations, resulting in the premature rear lock and decline in the utilization adhesion coefficient. To cope with this situation, the paper puts forward the control strategy of regenerative braking in the parallel composite braking system, which consists of the conventional fictional braking system and hydraulic regenerative braking system. The control strategy is revised according to the external character of the parallel composite braking system and ECE regulations. The simulation results demonstrate its effectiveness in improving the brake energy recovery in typical urban drive state.

2. Configuration of PHHV

This rear-wheel-drive hydraulic hybrid vehicle, shown in Figure 1, consists primarily of an internal combustion engine, a high pressure accumulator, low pressure reservoir, and a variable displacement hydraulic pump/motor unit. The primary power source is the same diesel engine used in the conventional vehicle. The transmission, propeller shaft, and the differential and driving shaft are the same as those in the conventional vehicle. The hydraulic pump/motor is coupled with the propeller shaft via a torque coupler [17, 18]. The basic parameters of the parallel hydraulic hybrid vehicle studied in this paper are as shown in Table 1.

During deceleration, the hydraulic pump/motor decelerates the vehicle while operating as a pump to capture the energy normally lost to friction brakes in a conventional vehicle. Also, when the vehicle brake is applied, the hydraulic pump/motor uses the braking energy to charge the hydraulic fluid from a low pressure hydraulic accumulator into a high-pressure accumulator, increasing the pressure of the nitrogen gas in the high pressure accumulator. The high pressure hydraulic fluid is used by the hydraulic pump/motor unit to generate torque during the next vehicle launch and acceleration [19–21]. It is designed and sized to capture braking energy from normal, moderate braking events and is supplemented by friction brakes for aggressive braking.

Ignoring the vehicle rolling resistance moment, the front wheel braking force F_{f1} and the rear wheel braking force F_{f2} are given by the following, respectively:

$$F_{f1} = \frac{\varphi\left(Gb + m\left(du/dt\right)h_g - \left(C_D A u^2/21.15\right)h_g\right)}{L}, \quad (1)$$

$$F_{f2} = \frac{\varphi\left(Ga - m\left(du/dt\right)h_g + \left(C_D A u^2/21.15\right)h_g\right)}{L}, \quad (2)$$

where φ is the adhesion coefficient between tire and road surface, G is the vehicle gravity (N), m is the vehicle quality (kg), a is the distance from vehicle center of gravity to front axle center line (m), b is the distance from vehicle center of gravity to rear axle center line (m), L is wheel base (m), h_g is the height of the center of gravity (m), C_D is the air resistance coefficient, A is the frontal area (m^2), u and is the vehicle speed (m/s).

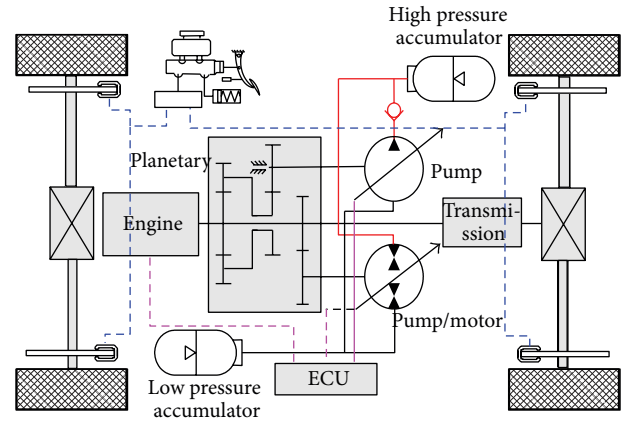

Figure 1: Configuration of PHHV.

Table 1: Basic parameters of PHHV.

Name	Parameter
Wheel radius	0.28 m
Maximum weight	1795 kg
Complete vehicle kerb mass	865 kg
Final drive axle ratio	4.129
Volume of the hydraulic accumulator	25 L
Filling pressure of the hydraulic accumulator	12 MPa
Maximum working pressure of the hydraulic accumulator	31 MPa
Minimum working pressure of the hydraulic accumulator	15 MPa
Torque coupler gear ratio	1.3
Hydraulic pump/motor capacity	A4VG56/56 mL/r

3. Design of Parallel Regenerative Braking Control Algorithm

During the composite braking, the brake severity is usually set at 0.1~0.7. After this phase, the regenerative braking force on the rear wheel, will rise, which will raise the utilization adhesion coefficient of the rear wheel whereas that of the front wheel goes down. As a result, the utilization adhesion coefficient on the rear wheel tends to surpass the constraint of ECE regulations, while the front wheel tends to be safer, with the possibility of lock being lowered in a further way.

In order to ensure the vehicle braking performance, ECE regulations demand the following: when the adhesion

coefficient φ is between 0.2 and 0.8, the braking severity is $z \geq 0.1 + 0.7(\varphi - 0.2)$; thus, the following is gained:

$$F_{xb2} \leq \frac{z + 0.04}{0.7} \frac{(a - zh_g) G}{L}, \qquad F_{xb1} = Gz - F_{xb2}. \tag{3}$$

As shown in Figure 2, the maximum rear wheel braking force curves are depicted in the wheel braking force distribution diagram, where line OC denotes line β, over which the ideal wheel braking force distribution line I lies. The vehicle synchronization adhesion coefficient is 0.75. The regulations can be satisfied with the ignorance of the regenerative braking system character. Line AB in the figure denotes the composite braking phase when the energy can be recovered to the largest degree, and OA is the biggest braking force during the pure regenerative braking. In order to prevent the premature lock of rear wheels during massive braking ($z > 0.7$) of the vehicle, the right boundary line goes down along with the line r where brake severity is 0.7, as is shown in Figure 2 as line BC.

In the composite braking phase shown in Figure 2, the braking force on front and rear wheels is as follows:

$$F_{xb2} = K(F_{xb1} + 0.115G) \quad (0.1 < z < z_B),$$
$$F_{xb2} = \frac{-0.7h_g}{L + 0.7h_g} F_{xb1} + \frac{0.7Gb}{L + 0.7h_g} \quad (z_B \leq z \leq 0.7), \tag{4}$$

where z_B is brake severity corresponding to point B, K is slope of line AB.

Here $K = 1.1407$, $z_B = 0.45$. After the revise according to points A and C, the limit values of braking severity z are 0.127 and 0.715. The regenerative braking force $F_{p/m}$ can be gained by the regenerative braking control algorithm:

$$F_{p/m} = \begin{cases} \dfrac{T_{p/m}}{r} = Gz, & z \leq 0.127, \\ Gz - \dfrac{G(z - 0.115K)}{(1 + K)\beta}, & 0.127 < z \leq z_B, \\ Gz - \dfrac{Gz(L + 0.7h_g) - 0.7Ga}{L\beta}, & z_B < z < 0.715. \end{cases} \tag{5}$$

After the concrete parameters of the hydraulic hybrid vehicle are input into the above equations, the relation in conditions of different brake severity and hydraulic accumulator pressure between regenerative braking system character and the algorithm distribution results is gained, which is depicted in Figure 3. As is shown in the figure, when hydraulic accumulator pressure is relatively lower and the brake severity $z \leq 0.1$ and $z \geq 0.5$, the regenerative braking distribution result is that the demanded regenerative braking force is lower than regenerative braking system character, proving that the regenerative braking power of the system has not been fully performed. In the phase of $0.1 < z < 0.5$, the regenerative braking power is far from the requirements of the algorithm. Therefore, it is necessary to add character constraint of the regenerative braking system.

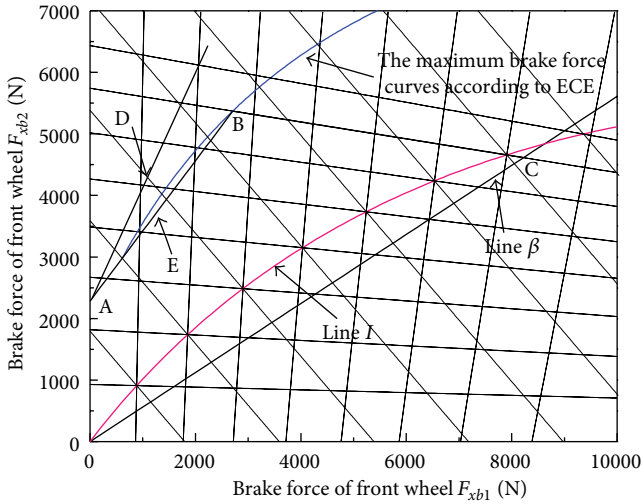

Figure 2: Brake force distribution curves of PHHV.

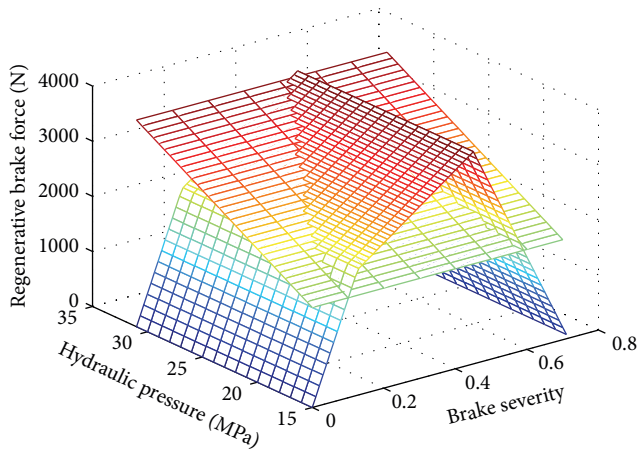

Figure 3: Relation between regenerative braking system character and algorithm distribution results.

4. The Parallel Regenerative Braking Control Algorithm Based on Regenerative Braking System Character and ECE Regulations

The regenerative braking force is linearly related with hydraulic accumulator pressure. Therefore, the basic thought of control algorithm is that before the distribution of each time the maximum braking power F_{p/m_max} of the regenerative braking system is confirmed according to the driving speed and hydraulic accumulator pressure; the pure regenerative braking is adopted when the total braking force demand F_{bd} corresponding to braking severity z meets the condition of $F_{bd} < F_{p/m\_max}$; otherwise, the composite braking is adopted. In the process of composite braking, the regenerative braking force will be preferential for use, and the frictional braking force will supplement the rest. The detailed process of algorithm distribution is as follows.

(1) According to target brake severity, the total braking force demand is calculated as $F_{bd} = Gz$. The maximum regenerative braking power F_{p/m_max} at the moment of the hydraulic pump/motor is gained by referring to the pressure phenomena of the accumulator.

(2) If $F_{p/m\_max} \geq F_{bd}$, the braking force will be fully provided by the hydraulic pump/motor, when $F_{p/m} = F_{bd}$ and both the front wheel frictional braking force F_f and the rear F_r will be 0.

(3) If $F_{p/m\_max} < F_{bd}$, the frictional braking force on front and rear wheels goes up along with line β, when the regenerative braking force is $F_{p/m} = F_{p/m\_max}$, the frictional braking force on rear wheels is $F_r = (1-\beta)(F_{bd}-F_{p/m\_max})$, and the hydraulic braking force on front wheels is $F_f = \beta(F_{bd} - F_{p/m\_max})$. Therefore, the regenerative braking force during braking can be gained and is shown in Figure 4, while the simultaneous simulation results of front and rear axle utilization coefficients are in Figure 5.

According to Figures 4 and 5, as the algorithm ensures the maximum regenerative braking power in the first place, the braking force distribution surpasses the constraint of ECE regulations, resulting in the necessity of adding ECE regulations constraints into the algorithm. After the calculation, the relation between the maximum limiting line of ECE regulations to rear wheel braking force and the front-rear force distribution line in the phase of the maximum algorithm regenerative braking force is shown in Figure 2.

It can be seen from Figure 2 that line AD which denotes the basic algorithm distribution is beyond ECE regulations. Thereby, taking point D, for example, the distribution results should be revised onto the point E intersected by ECE line and the corresponding equal-braking-severity line. The detailed revise algorithm is as follows.

(1) The regenerative braking power F_{p/m_max} should be gained from pressure phenomena of hydraulic accumulator by referring to the target brake severity z and the total braking force demand F_{bd}.

(2) If $F_{p/m\_max} \geq F_{bd}$, from the following equations

$$\begin{aligned} F_{xb2} &= K\left(F_{xb1} + 0.115G\right) \\ 0 &= Gz - F_{xb1}, \end{aligned} \tag{6}$$

$F_{xb2} = F_{xb2A}$ can be gained, where F_{xb2A} denotes the rear wheel braking force corresponding to point A.

If $F_{p/m\_max} \leq F_{xb2A}$, the braking force will be completely provided by regenerative braking, when the regenerative braking moment is $T_{p/m} = F_{bd}/r$ and the front wheel frictional braking force F_f and the rear F_r are both 0, which should be revised otherwise. The detail is as follows.

If $0 < z \leq 0.127$, the regenerative braking moment is $T_{p/m} = F_{bd}/r$ and both the front frictional braking force F_f and the rear F_r are 0.

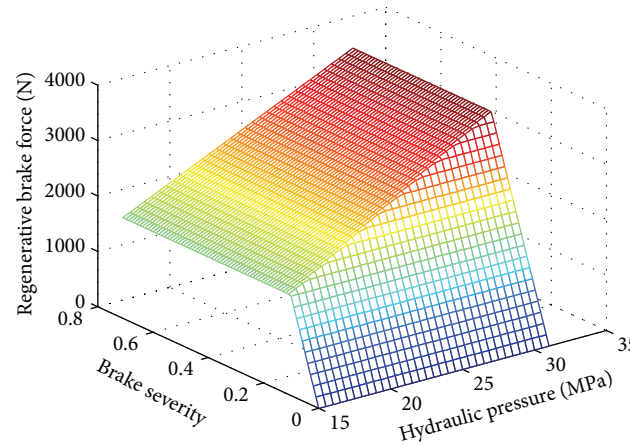

Figure 4: The results of the algorithm allocation based on the constrained regenerative braking system.

If $0.127 < z \leq 0.2$,

$$\begin{aligned} F_{xb2} &= K\left(F_{xb1} + 0.115G\right), \\ F_f &= F_{xb1} = Gz - F_{xb2}, \\ F_f &= \frac{\beta}{1-\beta}F_r, \\ F_m &= F_{bd} - F_r - F_f. \end{aligned} \tag{7}$$

If $0.2 < z \leq 0.45$,

$$\begin{aligned} F_{xb2} &= \frac{z+0.04}{0.7}\frac{\left(a - zh_g\right)G}{L}, \\ F_f &= F_{xb1} = Gz - F_{xb2}, \\ F_f &= \frac{\beta}{1-\beta}F_r, \\ F_m &= F_{bd} - F_r - F_f. \end{aligned} \tag{8}$$

If $0.45 < z \leq 0.715$,

$$\begin{aligned} F_{xb2} &= -\frac{0.7h_g}{L+0.7h_g}F_{xb1} + \frac{0.7Ga}{L+0.7h_g}, \\ F_f &= F_{xb1} = Gz - F_{xb2}, \\ F_f &= \frac{\beta}{1-\beta}F_r, \\ F_m &= F_{bd} - F_r - F_f. \end{aligned} \tag{9}$$

(3) If $F_{p/m\_max} < F_{bd}$, the predistributed front-rear wheel frictional braking force rises along line β. The regenerative braking force is $F_{p/m} = F_{p/m\_max}$, while the rear wheel frictional braking force is $F_r = (1-\beta)(F_{bd} - F_{p/m\_max})$ and the front is $F_f = \beta(F_{bd} - F_{p/m\_max})$.

If $0 < z \leq 0.127$, the regenerative braking force is $F_m = F_{max}$, while the rear wheel frictional braking force is $F_r = (1-\beta)(F_{bd} - F_{p/m\_max})$ and the front is $F_f = \beta(F_{bd} - F_{p/m\_max})$.

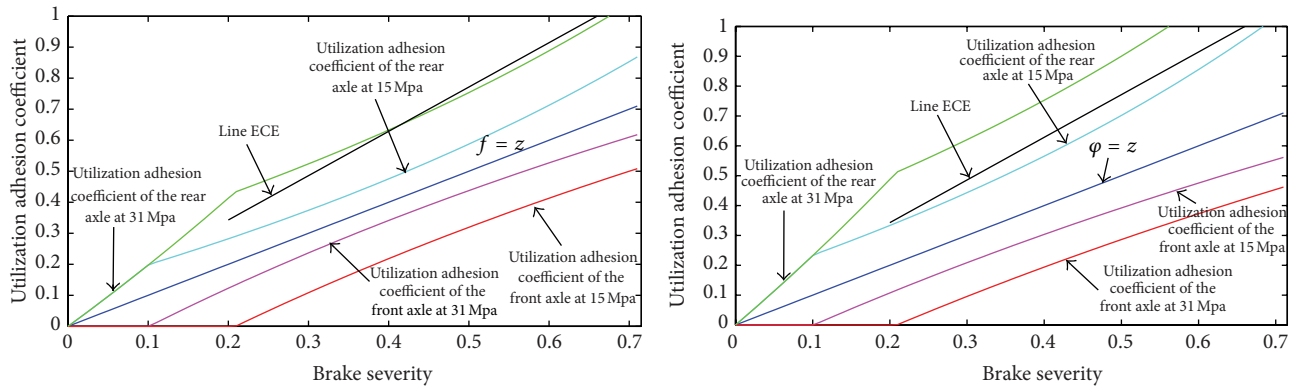

(a) Full load (b) Empty load

Figure 5: Simulation results of front and rear axle utilization coefficients.

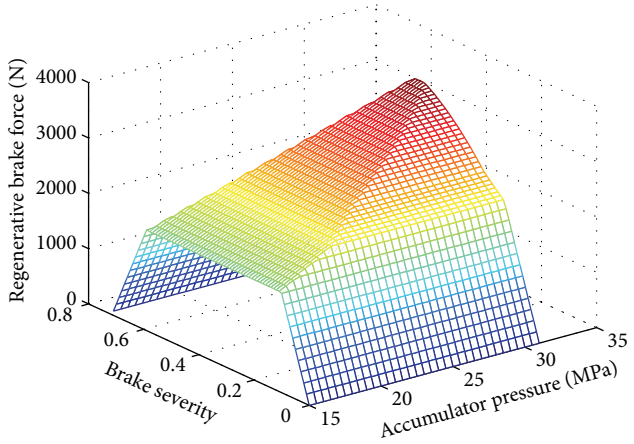

Figure 6: The results of braking force distribution revised according to ECE regulations.

If $0.127 < z \le 0.2$, from the equations

$$F_{xb2} = K\left(F_{xb1} + 0.115G\right),$$
$$F_{xb1} = Gz - F_{xb2}, \tag{10}$$

$F_{xb1} = F_{xb1E}$ can be gained, where F_{xb1E} denotes the front wheel braking force corresponding to point E. If the predistribution result is $F_f > F_{xb1E}$, the revise is not necessary, while this is needed otherwise. The revise results are as follows

$$F_{xb2} = K\left(F_{xb1} + 0.115G\right),$$
$$F_f = F_{xb1} = Gz - F_{xb2},$$
$$F_f = \frac{\beta}{1-\beta}F_r, \tag{11}$$
$$F_{p/m} = F_{bd} - F_r - F_f.$$

If $0.2 < z \le 0.45$, from the equations

$$F_{xb2} = \frac{z + 0.04}{0.7}\frac{\left(a - zh_g\right)G}{L},$$
$$F_f = F_{xb1} = Gz - F_{xb2}, \tag{12}$$

$F_{xb1} = F_{xb1E}$ can be gained, where F_{xb1E} denotes the front wheel braking force corresponding to point E. If the predistribution result is $F_f > F_{xb1E}$, the revise is not necessary, while this is needed otherwise. The revise results are as follows

$$F_{xb2} = \frac{z + 0.04}{0.7}\frac{\left(a - zh_g\right)G}{L},$$
$$F_f = F_{xb1} = Gz - F_{xb2},$$
$$F_f = \frac{\beta}{1-\beta}F_r, \tag{13}$$
$$F_{p/m} = F_{bd} - F_r - F_f.$$

If $0.45 < z \le 0.715$, from the equations

$$F_{xb2} = \frac{-0.7h_g}{L + 0.7h_g}F_{xb1} + \frac{0.7Ga}{L + 0.7h_g},$$
$$F_f = F_{xb1} = Gz - F_{xb2}, \tag{14}$$

$F_{xb1} = F_{xb1E}$ can be gained, where F_{xb1E} denotes the front wheel braking force corresponding to point E. If the predistribution result is $F_f > F_{xb1E}$, the revise is not necessary, while this is needed otherwise. The revise results are as follows

$$F_{xb2} = \frac{-0.7h_g}{L + 0.7h_g}F_{xb1} + \frac{0.7Ga}{L + 0.7h_g},$$
$$F_f = F_{xb1} = Gz - F_{xb2},$$
$$F_f = \frac{\beta}{1-\beta}F_r, \tag{15}$$
$$F_{p/m} = F_{bd} - F_r - F_f.$$

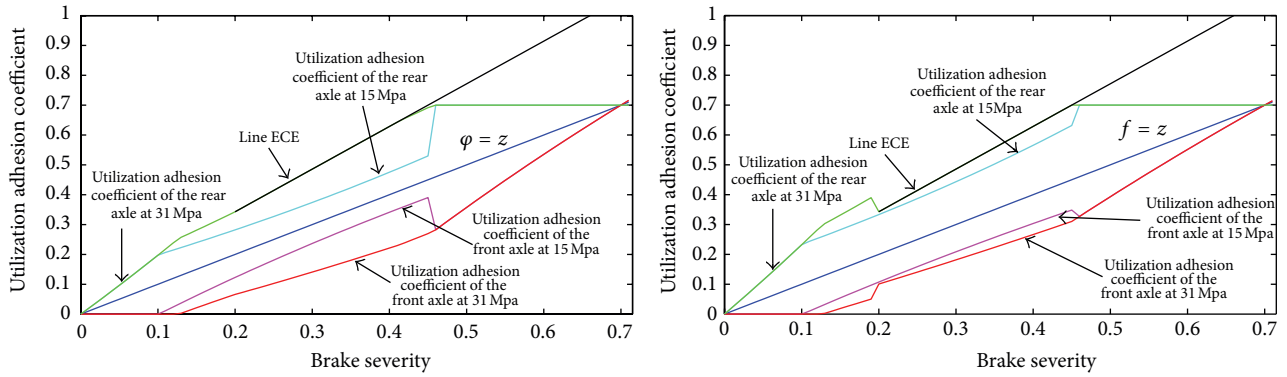

(a) Full load (b) Empty load

Figure 7: Simulation results of revised front and rear axle utilization coefficients.

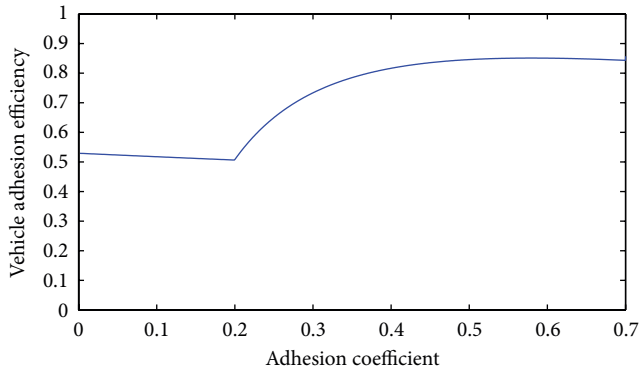

Figure 8: The vehicle adhesion efficiency based on parallel regenerative braking.

The results of braking force distribution revised according to ECE regulations are shown in Figure 6, and the utilization adhesion coefficient curves are shown in Figure 7.

The comparisons between Figures 4 and 6 as well as Figures 5 and 7 show that the revised zone is relatively large and the distribution results after revise can satisfy the requirements of both regenerative braking system and ECE regulations.

According to Figure 2 which tells the distribution phenomena, on the condition of the remaining braking force ratio β, ECE regulation limits can be easily exceeded if the parallel regenerative braking control algorithm without revise by ECE is adopted, aiming to fully perform the regenerative braking power. Although the braking force distribution results revised according to ECE regulations meet the requirement of the regulations, the braking energy recovery efficiency is affected, however, resulting in the necessity of rematch to the braking force ratio β to improve the safety and energy recovery efficiency of hydraulic hybrid vehicles.

According to Figure 7, in order to recover the braking energy to the largest degree, the rear axle will be preferentially exerted on regenerative braking force; thus, the utilization adhesion coefficient on the rear axle is above that of the front. Therefore, the rear wheels will lock every time before the front ones, which is a dangerous condition. Hence, the hybrid vehicle driven by rear wheels must be equipped with ABS (antilock brake system), which controls the performance of regenerative braking system. At the same time, however, the vehicle adhesion efficiency should satisfy the requirement of regulations of $\varepsilon \geq 0.75$.

The vehicle adhesion efficiency when braking is depicted in Figure 8. When the vehicle brakes on the road with extralow adhesion coefficient (below 0.3 in the figure), the adhesion efficiency will be $\varepsilon < 0.75$. Therefore, if the road adhesion coefficient is lower than 0.3, the parallel composite braking system will checkout the information about the road adhesion phenomenon though ABS and the regenerative braking system controller, and then it stops exerting regenerative braking force at the right time.

5. Simulation Research

Vehicle control model is the core of control strategy. Based on the requirement of driving cycle, the total torques are distributed among engine, hydraulic accumulator, hydraulic pump/motor, and the friction brake system reasonably. Vehicle control model consists of regenerative braking system, energy release system, and active stamping system, as shown in Figure 9.

Based on the algorithm above, the model of braking force distribution on hydraulic hybrid vehicles is set up in Matlab/Simulink and shown in Figure 10.

In order to verify the rationality and validity of the regenerative braking strategy discussed in this chapter, the parallel regenerative braking control strategy is adopted, and 1015, NYCC, and UDDS drive states are chosen to make the simulation study of brake energy recovery. After the road being set with high adhesion coefficient, the simulation results are achieved and shown in Table 2. Meanwhile the results of the evaluation of driving cycles with strategy of the ADVISOR in [22] are cited and shown in Table 3.

According to Table 2, the control strategy of regenerative braking in the hydraulic hybrid vehicle discussed in this

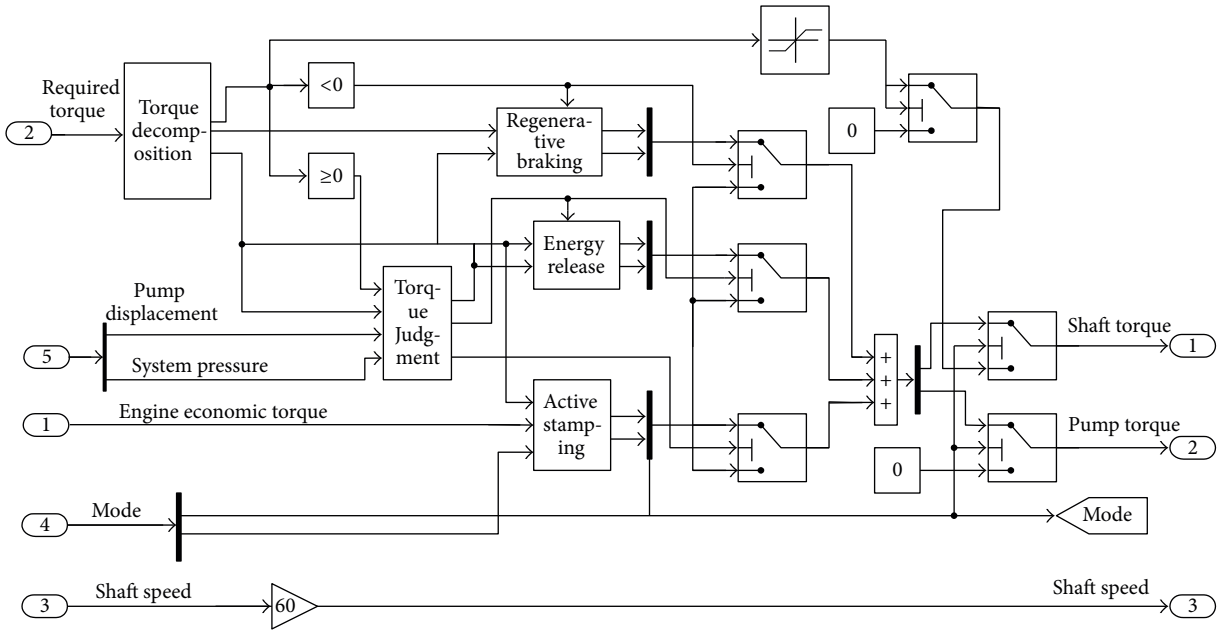

Figure 9: Top-level diagram of vehicle control model.

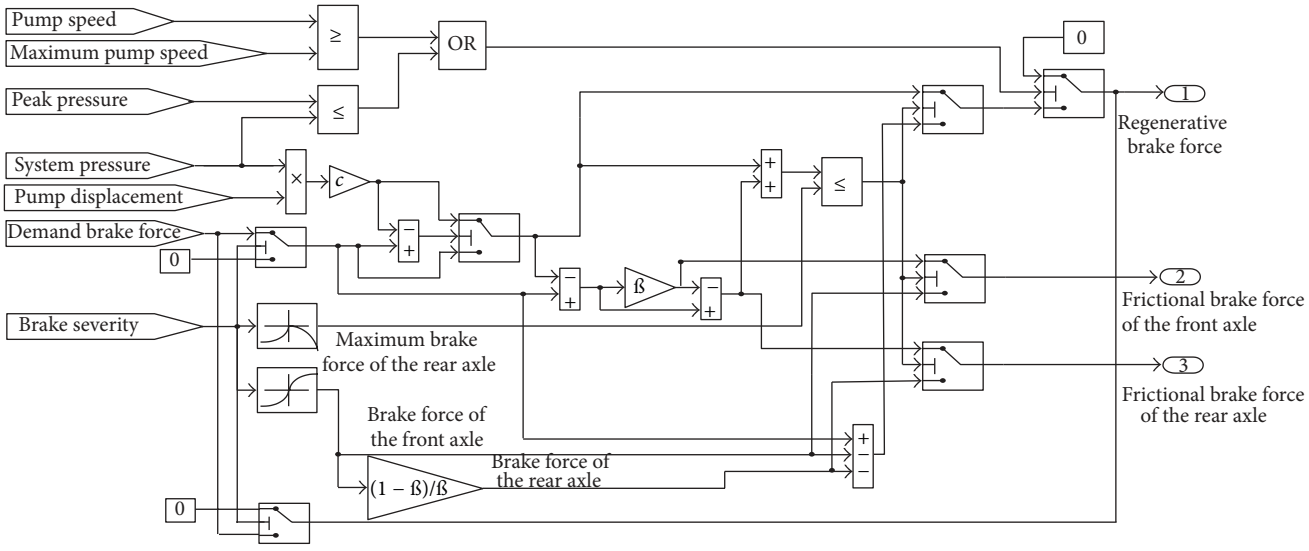

Figure 10: Model of braking force distribution of parallel regenerative braking.

paper can achieve the brake energy recovery to the largest degree based on the brake security. The brake energy recovery efficiency in 1015, NYCC, and UDDS is, respectively, 73.5% 75.25%, and 60.60%.

Compare the results in Table 2 with those in Table 3; it is not hard to find that the control strategy of regenerative braking in the hydraulic hybrid vehicle discussed in this paper can achieve more brake energy recovery than the strategy of the ADVISOR cited in [22].

6. Conclusions

Based on the higher power density and lower energy density of the hydraulic accumulator as well as the characteristics of the urban state, this paper puts forward the control algorithm of parallel composite braking in the hydraulic hybrid vehicle driven by rear wheels. By means of revise, the composite braking was controlled just within the requirements of ECE regulations. Therefore, based on the ensured brake security,

Table 2: The results of brake energy recovery rate in different drive states with the proposed strategy.

Drive state	Average acceleration a_{avg} (m·s^{-2})	Brake severity $z \leq 0.1$ (%)	Brake energy E_r (kWh)	Brake energy recovery rate ε_r (%)
1015	0.57/−0.65	96.2	0.2256	73.5
NYCC	0.62/−0.61	75.5	0.04	75.25
UDDS	0.51/−0.58	74.5	2.731	60.60

Table 3: The results of the evaluation of driving cycles with strategy of the ADVISOR.

Drive state	Traveling distance (Km)	Brake energy (kJ)	Regenerative braking efficient (kJ)	Brake energy recovery rate (%)
1015	4.2	660	367	56
NYCC	1.9	614	302	49
UDDS	12	1856	1017	55

the algorithm designed can enlarge the regenerative braking ratio to the utmost in the phase of composite braking, improving the brake energy recovery power of the vehicle at the end.

Acknowledgments

This work was supported by National Natural Science Foundation of China and Natural Science Foundation of Shandong Province under Contracts no. 50875054 and no. ZR2009FL002.

References

[1] W. Gunselman, "Technologies for increased energy efficiency in railway systems," in *Proceedings of the 11th European Conference on Power Electronics and Applications*, pp. 1–10, 2005.

[2] K. Son, S. Noh, K. Kwon, J. Choi, and E. K. Lee, "Line voltage regulation of urban transit systems using supercapacitors," in *Proceedings of the IEEE 6th International Power Electronics and Motion Control Conference (IPEMC '09)*, pp. 933–938, May 2009.

[3] K. Matsuda, H. Ko, and M. Miyatake, "Train operation minimizing energy consumption in dc electric railway with onboard energy storage device," in *Power Supply, Energy Management and Catenary Problems Part A*, pp. 45–54, WIT Press, Southampton, UK, 2010.

[4] T. Konishi, H. Morimoto, T. Aihara, and M. Tsutakawa, "Fixed energy storage technology applied for DC Electrified railway," *IEEJ Transactions on Electrical and Electronic Engineering*, vol. 5, no. 3, pp. 270–277, 2010.

[5] M. Ogasa, "Application of energy storage technologies for electric railway vehicles-examples with hybrid electric railway vehicles," *IEEJ Transactions on Electrical and Electronic Engineering*, vol. 5, no. 3, pp. 304–311, 2010.

[6] D. Kim, S. Hwang, and H. Kim, "Vehicle stability enhancement of four-wheel-drive hybrid electric vehicle using rear motor control," *IEEE Transactions on Vehicular Technology*, vol. 57, no. 2, pp. 727–735, 2008.

[7] D. Peng, Y. Zhang, C. L. Yin, and J. W. Zhang, "Combined control of a regenerative braking and antilock braking system for hybrid electric vehicles," *International Journal of Automotive Technology*, vol. 9, no. 6, pp. 749–757, 2008.

[8] K. Oh, D. Kim, T. Kim, C. Kim, and H. Kim, "Operation algorithm for a parallel hybrid electric vehicle with a relatively small electric motor," *KSME International Journal*, vol. 18, no. 1, pp. 30–36, 2004.

[9] C. Jo, J. Ko, H. Yeo, T. Yeo, S. Hwang, and H. Kim, "Cooperative regenerative braking control algorithm for an automatic-transmission-based hybrid electric vehicle during a downshift," *Proceedings of the Institution of Mechanical Engineers, Part D: Journal of Automobile Engineering*, vol. 226, no. 4, pp. 457–467, 2012.

[10] J. Zhang, C. Lv, J. Gou, and D. Kong, "Cooperative control of regenerative braking and hydraulic braking of an electrified passenger car," *Proceedings of the Institution of Mechanical Engineers, Part D: Journal of Automobile Engineering*, vol. 226, no. 10, pp. 1289–1302, 2012.

[11] J. Moreno, M. E. Ortúzar, and J. W. Dixon, "Energy-management system for a hybrid electric vehicle, using ultracapacitors and neural networks," *IEEE Transactions on Industrial Electronics*, vol. 53, no. 2, pp. 614–623, 2006.

[12] P. Wu, N. Luo, F. J. Fronczak, and N. H. Beachley, "Fuel economy and operating characteristics of a hydropneumatic energy storage automobile," SAE Paper 851678, 1985.

[13] S. Hui, J. Ji-hai, and W. Xin, "Torque control strategy for a parallel hydraulic hybrid vehicle," *Journal of Terramechanics*, vol. 46, no. 6, pp. 259–265, 2009.

[14] A. Taghavipour, M. S. Foumani, and M. Boroushaki, "Implementation of an optimal control strategy for a hydraulic hybrid vehicle using CMAC and RBF networks," *Scientia Iranica*, vol. 19, no. 2, pp. 327–334, 2012.

[15] S. Hui, "Multi-objective optimization for hydraulic hybrid vehicle based on adaptive simulated annealing genetic algorithm," *Engineering Applications of Artificial Intelligence*, vol. 23, no. 1, pp. 27–33, 2010.

[16] R. Ramakrishnan, S. S. Hiremath, and M. Singaperumal, "Theoretical investigations on the effect of system parameters in series hydraulic hybrid system with hydrostatic regenerative braking," *Journal of Mechanical Science and Technology*, vol. 26, no. 5, pp. 1321–1331, 2012.

[17] R. P. Kepner, "Hydraulic power assist—a demonstration of hydraulic hybrid vehicle regenerative braking in a road vehicle application," SAE Paper 2002-01-3128, 2002.

[18] T. Liu, J. Jiang, and H. Sun, "Investigation to simulation of regenerative braking for parallel hydraulic hybrid vehicles,"

in *Proceedings of the International Conference on Measuring Technology and Mechatronics Automation (ICMTMA '09)*, pp. 242–245, April 2009.

[19] Y. J. Kim and Z. Filipi, "Simulation study of a series hydraulic hybrid propulsion system for a light truck," SAE Paper 2007-01-4151, 2007.

[20] R. P. Kepner, "Hydraulic power assist—a demonstration of hydraulic hybrid vehicle regenerative braking in a road vehicle application," SAE Paper 2002-01-3128.

[21] M. Paul and S. Jacek, "Development and simulation of a hydraulic-hybrid powertrain for use in commercial heavy vehicles," SAE Paper 2003-01-3370.

[22] L. Chu, M. Shang, Y. Fang, J. Guo, and F. Zhou, "Braking force distribution strategy for HEV based on braking strength," in *Proceedings of the International Conference on Measuring Technology and Mechatronics Automation (ICMTMA '10)*, pp. 759–764, March 2010.